Cancer Research

Effect of Estrogen Withdrawal on Energy-rich Phosphates and Prediction of Estrogen Dependence Monitored by *in Vivo* ^{31}P Magnetic Resonance Spectroscopy of Four Human Breast Cancer Xenografts

Claus A. Kristensen, Paul E. G. Kristjansen, Nils Brünner, et al.

Cancer Res 1995;55:1664-1669.

[CANCER RESEARCH 55, 1664–1669, April 15, 1995]

Effect of Estrogen Withdrawal on Energy-rich Phosphates and Prediction of Estrogen Dependence Monitored by *in Vivo* ^{31}P Magnetic Resonance Spectroscopy of Four Human Breast Cancer Xenografts[1]

Claus A. Kristensen,[2] Paul E. G. Kristjansen, Nils Brünner, Robert Clarke, Mogens Spang-Thomsen, and Bjørn Quistorff

The Finsen Center, National University Hospital [C. A. K., P. E. G. K., N. B.], Institute of Pathological Anatomy [C. A. K., P. E. G. K., M. S-T.], and NMR-Center [B. Q.], University of Copenhagen, Copenhagen, Denmark and Vincent Lombardi Cancer Research Center, Georgetown University Medical School, Washington, DC 20007 [R. C.]

ABSTRACT

The effect of estrogen withdrawal on energy metabolism was studied in four human breast cancer xenografts: the estrogen-dependent MCF-7 and ZR75-1 and the estrogen-independent ZR75/LCC-3 and MDA-MB-231. The tumors were grown in ovariectomized nude mice with a s.c. implanted estrogen pellet. After Gompertzian growth was verified, the estrogen pellet was removed from half of the animals. *In vivo* ^{31}P magnetic resonance spectroscopy of the tumors was performed 1 day before and on days 2, 6, and 14 after estrogen removal. Estrogen withdrawal induced a significant increase in the nucleoside triphosphate:P_i ratio in the two estrogen-dependent xenografts, whereas this ratio remained unchanged in the estrogen-independent tumors. In ZR75/LCC-3 tumors a slight decrease in nuceloside triphosphate:P_i was observed following onset of estrogen stimulation after initial growth without estrogen. Extracts of freeze-clamped tumors prepared 14 days after estrogen removal were analyzed for ATP and phosphocreatine content. Our findings suggest a correlation between estrogen withdrawal and the steady-state concentrations of ATP, phosphocreatine, and P_i in human breast cancer xenografts. Discrimination analysis of the pretherapeutic spectra enabled us to identify the tumor line and the estrogen dependence of the tumors in 80–90% of all cases.

INTRODUCTION

The antiproliferative effect of estrogen withdrawal or antiestrogen therapy has been used clinically for decades, but only little is known about the influence of this treatment on cellular energy metabolism. Noninvasive ^{31}P-MRS[3] studies of tumor tissue *in vitro* and *in vivo* provide information about energy and phospholipid metabolism in malignant cells and tissues. The data are usually expressed as ratios of metabolites (*e.g.*, NTP:P_i, PME:P_i, and PCr:NTP). Pretherapeutic ratios as well as the course of changes after initiation of anticancer therapy have been suggested as possible parameters for early response prediction and monitoring (1, 2).

The aims of the present study were to evaluate the influence of estrogen withdrawal on energy-rich phosphates in human breast tumor xenografts, and to examine the potential of the ^{31}P MRS profile in prediction of estrogen sensitivity. Four different human breast tumor lines were included: two estrogen receptor positive/estrogen dependent (MCF-7 and ZR75-1) and two estrogen receptor negative/estrogen independent (ZR75/LCC-3 and MDA-MB-231). ZR75/LCC-3 is a subline of the estrogen-dependent ZR75–1, selected for *in vivo* estrogen independence.[4]

Estrogen withdrawal induced a significant increase in the NTP:P_i ratio in both of the estrogen-dependent tumor lines. Similar effects have been observed by others in MCF-7 tumors following initiation of tamoxifen therapy and concurrent withdrawal of estrogen (3, 4). Our study suggests that the increase in NTP:P_i is due to estrogen withdrawal alone. In the estrogen-independent tumors estrogen withdrawal had no influence on NTP:P_i.

The use of a linear discriminant function in the analysis of the NTP:P_i, PME:P_i PDE:P_i, PME:NTP, and PCr:NTP ratios enabled a correct assessment of the estrogen dependence of the tumors in 80–90% of all cases.

MATERIALS AND METHODS

Tumors. Four cell lines were established as solid tumor xenografts in nude mice: the estrogen-dependent, estrogen receptor-positive tumor lines MCF-7 and ZR75-1 as well as the corresponding estrogen-independent, receptor-negative subline ZR75/LCC-3 and the estrogen-independent, receptor-negative MDA-MB-231 line.

ZR75/LCC-3 was established by injection of ZR75-1 cells into ovariectomized nude mice. Three months later several of the animals had developed small tumors. One of the tumors was excised and reestablished in culture with IMEM without phenol red and supplemented with 5% CCS. The resulting cell line was named ZR75/LCC-3.

MCF-7, MDA-MB-231, and ZR-75-1 were routinely grown in IMEM with phenol red containing 5% FCS, while ZR-75–1/LCC-3 was routinely carried in IMEM without phenol red and supplemented with 5% CCS. Serum was stripped of endogenous steroids by treatment with dextran-coated charcoal and sulfatase as described previously (5). Cells were harvested at about 80% confluency using a cell scraper, and subsequently 2×10^6 cells were inoculated into each flank of 8–10-week-old ovariectomized NMRI *nu/nu* athymic nude mice (BOMMICE, Ry, Denmark). The mice carrying estrogen-dependent tumors received an 17β-estradiol pellet (60-day release, 0.72 mg; Innovative Research, Toledo, OH) s.c. at the time of inoculation. Growing tumors were excised, cut into 1-mm^3 pieces, and each of the four tumor lines were serially transplanted to a minimum of 16 ovariectomized mice for each experiment. All four tumor lines were serially maintained as xenografts.

Experimental Design. A minimum of 16 tumors of each type were allowed to grow during estrogen supplementation from a s.c. pellet until they reached a size of at least 10 mm in diameter (day 0). The estrogen pellet was removed from half of the animals by skin incision on day 0. ^{31}P MRS was performed on days −1, 2, 6, and 14. In a separate experiment, a series of ZR75/LCC-3 tumors were grown initially without 17β-estradiol supplementation and when the tumors had reached a minimum diameter of 10 mm (day 0), half of the animals received estrogen supplementation. MRS was performed in the same intervals as described above.

***In Vivo* ^{31}P MRS.** The mice were briefly anesthetized for 4–6 min with propanidide i.p. (Sombrevin, 500 mg/kg; Gideon Richter, Budapest, Hungary) and placed in a flexible PVC tube with the tumor protruding through a hole concentric with the radiofrequency coil. To provide exact fixation, the tail of the animal was taped to the tube. In this setup, the breathing movements were not transmitted to the tumor. During the spectral recording, the mice were restrained, but unanesthetized. A 14-mm two-turn surface coil was located

Received 9/26/94; accepted 2/16/95.

The costs of publication of this article were defrayed in part by the payment of page charges. This article must therefore be hereby marked *advertisement* in accordance with 18 U.S.C. Section 1734 solely to indicate this fact.

[1] This work was supported by grants from The Haensch Foundation, The Skovgaard Foundation, and The Danish Cancer Research Foundation.

[2] To whom requests for reprints should be addressed, at Department of Oncology ONK 5074, Rigshospitalet, Blegdamsvej 9, DK-2100 Copenhagen, Denmark.

[3] The abbreviations used are: MRS, magnetic resonance spectroscopy; E_2, 17β-estradiol; IMEM, improved minimal essential medium; NTP, nucleoside triphosphate; PCr, phosphocreatine; PDE, phosphodiesters; PME, phosphomonoesters; NMR, nuclear magnetic resonance; CCS, charcoal-stripped calf serum.

[4] Manuscript in preparation.

Table 1 *Classification of tumor lines according to the discrimination function*[a]

17β-Estradiol dependence	Tumor line	No. of tumors classified as MCF-7	No. of tumors classified as ZR75-1	No. of tumors classified as ZR75/LCC-3	No. of tumors classified as MDA-MB-231	Total	Predictability of estrogen dependence/independence
+	MCF-7	16/21[b] (76%)	1	2	2	21	36/44[c] (82%)
	ZR75-1	2	19/23[b] (83%)	2	0	23	
−	ZR75-1/LCC-3	2	0	20/22[b] (91%)	0	22	45/48[c] (94%)
	MDA-MB-231	1	0	1	24/26[b] (92%)	26	

[a] The predictability of tumor line and estrogen dependence/independence using linear discrimination function is based on the five ratios: NTP:P_i, PME:P_i, PDE:P_i, PME:NTP, and PCr:NTP.
[b] Correctly classified tumors.
[c] Number of tumors correctly discriminated out of the total number of tumors in the group (percentages in parentheses).

Table 2 *Prediction strength for each of the five ratios regarding estrogen independence*

Ratio	Predictability of estrogen independence	Cumulated predictability of estrogen independence	r^{2a}
PME:P_i	41/48 (85%)	41/48 (85%)	0.35
PME:NTP	34/48 (71%)	41/48 (85%)	0.09
PDE:P_i	39/48 (81%)	43/48 (90%)	0.13
PCr:NTP	22/48 (46%)	45/48 (94%)	0.10
NTP:P_i	36/48 (75%)	—[b]	—[b]

[a] r^2 = squared partial correlation coefficient: relative importance of the individual variable in the discrimination function.
[b] This parameter was not included in the forward selection due to a close correlation between NTP:P_i and PME:P_i (correlation coefficient, 0.8).

over the tumor in a special probe. A Vivospec spectrometer (Otsuka Electronics, Inc.) with a wide-bore 4.7 T magnet (Magnex, Inc.) was used. Sixty-four scans were acquired with a 10-s repetition time; these parameters ensured an acceptable signal:noise ratio and no signal saturation. The applied pulse width was 16 μs, corresponding to a flip angle of approximately 70°. The ratios were calculated from the area under the curve of each peak. The PCr:NTP ratios of the spectra did not differ from the corresponding enzymatically determined ratios.

Tumor Extracts. After the spectroscopic examination on day 14, tumors were freeze-clamped *in situ* following detachment from skin and other adherent tissues, but with intact vessels, applying a procedure described elsewhere (6). The subsequent weighing, perchloric acid extraction, and neutralization to pH 7.00 were performed according to procedures previously described (7). ATP and PCr were measured by enzymatic assays (8). The concentration unit applied is mmol/g tissue (wet weight).

Growth Curves. Mean tumor growth curves were constructed according to a transformed Gompertz function as described (9).

Statistical Analysis. To evaluate whether the five pretherapeutic ratios (NTP:P_i, PME:P_i, PDE:P_i, PME:NTP, and PCr:NTP) could distinguish among the four tumor lines, the following analysis was performed. Assuming each tumor line to have a multivariate normal distribution of the parameters measured, a discrimination function was estimated using a measure of generalized square distance. Subsequently the discrimination function was used for classification of each tumor into tumor line and ± estrogen dependence (Table 1). In the discrimination between the four tumor lines all five variables were included in the analysis. In order to estimate the relative importance of each of the ratios (Table 2), we used forward selection to choose the best subset of variables for estimation of the discrimination function. The calculations were performed using the SAS system (SAS Institute, Inc., Cary, NC).

In order to account for intertumoral variation, comparison of the sequence of spectra from each individual tumor was done by normalizing the metabolic ratios obtained during the 14-day time course to a fraction of the individual pretherapeutic value on day −1. The normalized ratios in the treated *versus* the control group were compared for each time point by the two-sided Wilcoxon test, since we could not assume a normal distribution of the ratio values abruptly changed by estrogen withdrawal. The same statistical test was used for the tumor extract data.

RESULTS

Estrogen Withdrawal. Estrogen withdrawal resulted in a marked increase in NTP:P_i ratio in the estrogen-dependent tumors ($P < 0.01$), whereas no significant differences occurred in the estrogen-independent tumors (Figs. 1–5). Typical spectra of ZR75-1 on days −1, 2, 6, and 14 are shown in Fig. 5, where the sharp increase in NTP:P_i from day 2 and forward is clearly visible. When ZR75/LCC-3 was grown initially without estrogen stimulation, the growth curve did not change after estrogen supplementation, and the trend toward a decrease in the NTP:P_i ratio of the estrogen-stimulated tumors was found to be statistically insignificant ($0.05 \leq P < 0.1$; Fig. 6).

The PCr:NTP ratio was only assessed in the ZR75-1 and ZR75/LCC-3 tumors, since most of the MDA-MB-231 and MCF-7 tumor spectra contained PCr levels below the MRS detection limit. In ZR75-1, estrogen withdrawal resulted in a constant PCr:NTP ratio of approximately 100% of the initial value during the whole 14-day time point, while the continuously estrogen-stimulated tumors had a markedly decreased PCr:NTP ratio on day 14 ($P < 0.025$; Fig. 2). No difference in the PCr:NTP ratio between estrogen-stimulated and estrogen-deprived ZR75/LCC-3 tumors was found; however, these tumors were not MRS analyzed on day 14 (Fig. 3).

In the tissue extracts (Table 3), no difference in tumor ATP content between the estrogen-stimulated and the estrogen-deprived ZR75–1 tumors was found. A clear increase in PCr content was observed when ZR75-1 as well as MCF-7 was estrogen deprived. This difference corresponds to the decrease in PCr:ATP during continuous estrogen stimulation demonstrated by ^{31}P MRS of ZR75-1 (Fig. 3) and is probably reflecting a decrease in PCr content following increasing ischemia during tumor growth. The estrogen-supplemented ZR75/

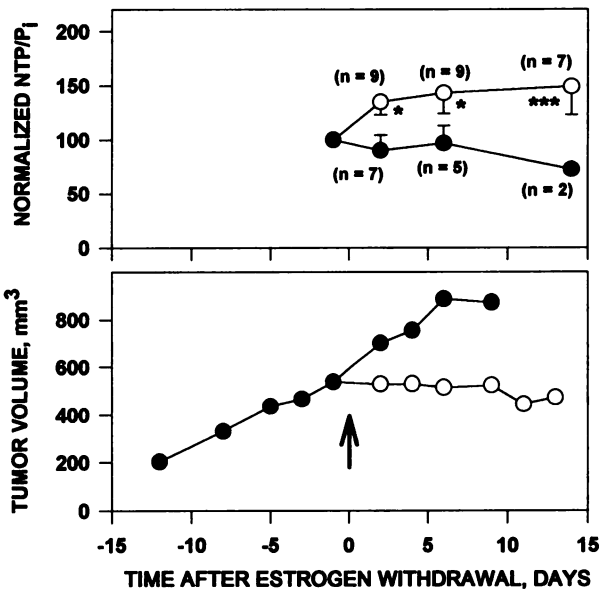

Fig. 1. Change in NTP:P_i (*top*) and growth curves (*bottom*) in MCF-7 tumors during 17β-estradiol stimulation (●) and after 17β-estradiol withdrawal (○). *Error bars*, upper and lower interquartile range. *Arrow*, day of estrogen withdrawal. *, $P < 0.01$, ***, $P \leq 0.05$.

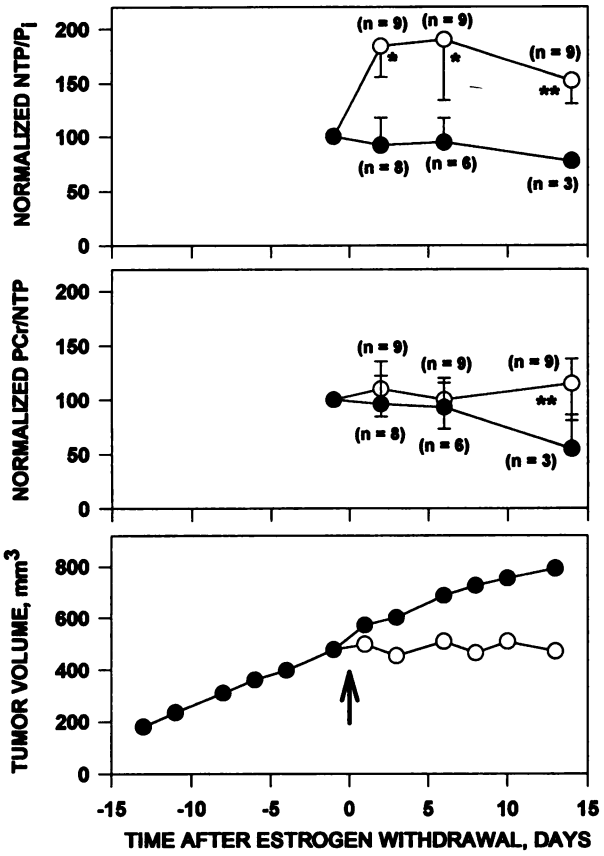

Fig. 2. Change in NTP:P$_i$ (*top*), PCr:NTP (*middle*), and growth curves (*bottom*) in ZR75-1 tumors during 17β-estradiol stimulation (●) and after 17β-estradiol withdrawal (○). *Error bars*, upper and lower interquartile range. *Arrow*, day of estrogen withdrawal. *, $P < 0.01$, **, $P \leq 0.025$.

LCC-3 tumors were characterized by a significantly lower ATP concentration than the estrogen-deprived tumors ($P < 0.01$). This difference was also found in MCF-7, but the amount of ATP/g tumor tissue in both MCF-7 groups was between 2 and 4 μg/g, whereas in the ZR75/LCC-3 tumors the ATP concentration was approximately 10 times lower in the estrogen-deprived tumors compared to the continuously stimulated tumors. Very low levels of PCr were found and there was no difference in ATP and PCr concentrations in the MDA-MB-231 tumors when comparing ± estrogen stimulation.

Classification of Tumor Lines. Pretherapeutic ratios and doubling time for the four examined tumors are presented in Fig. 7. Pretherapeutic ratios from all four tumor types were analyzed by the linear discriminant function. Table 1 shows the accuracy by which we were able to correctly classify the individual tumors and to predict the estrogen dependence and estrogen independence of the tumors. Also, the correctly classified tumors and the distribution of the misclassified tumors are given. Interestingly, there was no general pattern in the relatively infrequent misclassification of tumors: one estrogen-dependent line was not classified as the other estrogen-dependent line more frequently than as one of the estrogen-independent lines or *vice versa*. Since none of the 22 ZR75/LCC-3 tumors were classified as ZR75-1, there was no tendency to misclassify the estrogen-independent subline as the estrogen-dependent wild type. In Table 2 the relative importance of the five ratios with regard to their predictability of estrogen independence is given. PME:P$_i$ was the most important single contributor to the predictability of estrogen dependence on the basis of ^{31}P MRS. NTP:P$_i$ was the second most important single parameter but, due to a very close correlation (correlation coefficient, 0.8) between these two ratios, the SAS program demands that one of the two ratios are excluded in the performance of a discrimination involving several ratios. Since PME:P$_i$ is in itself the most important ratio, we chose to exclude NTP:P$_i$. Although the difference in PME:P$_i$ between ZR75/LCC-3 (with the highest ratio of the two estrogen-independent tumors) and MCF-7 (with the lowest ratio of

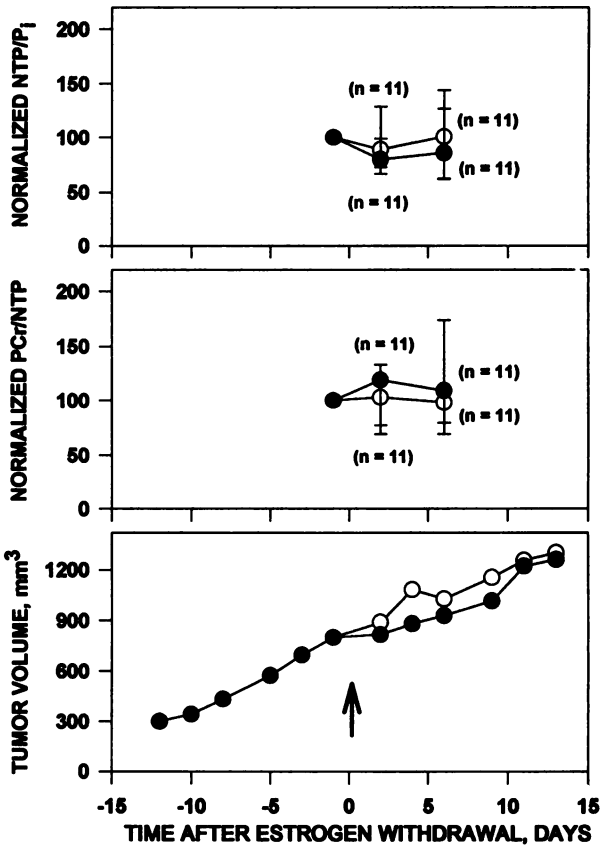

Fig. 3. Change in NTP:P$_i$ (*top*), PCr:NTP (*middle*), and growth curves (*bottom*) in ZR75/LCC-3 tumors during 17β-estradiol stimulation (●) and after 17β-estradiol withdrawal (○). *Error bars*, interquartile range. *Arrow*, day of estrogen withdrawal.

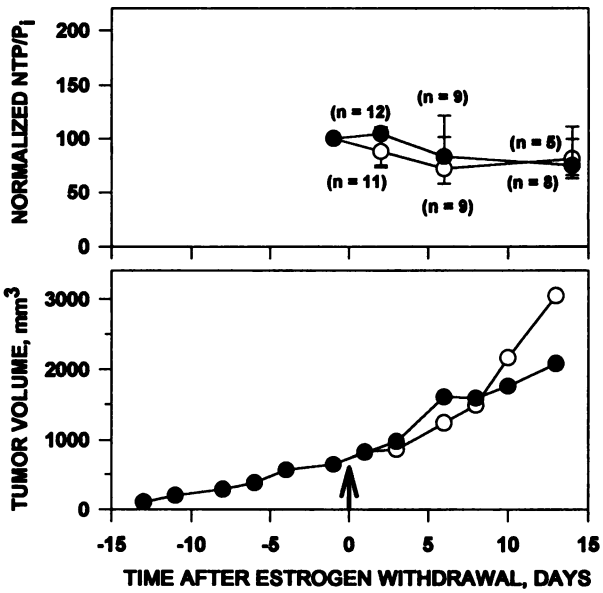

Fig. 4. Change in NTP:P$_i$ (*top*) and growth curves (*bottom*) in MDA-MB-231 tumors during 17β-estradiol stimulation (●) and after 17β-estradiol withdrawal (○). *Error bars*, interquartile range. *Arrow*, day of estrogen withdrawal.

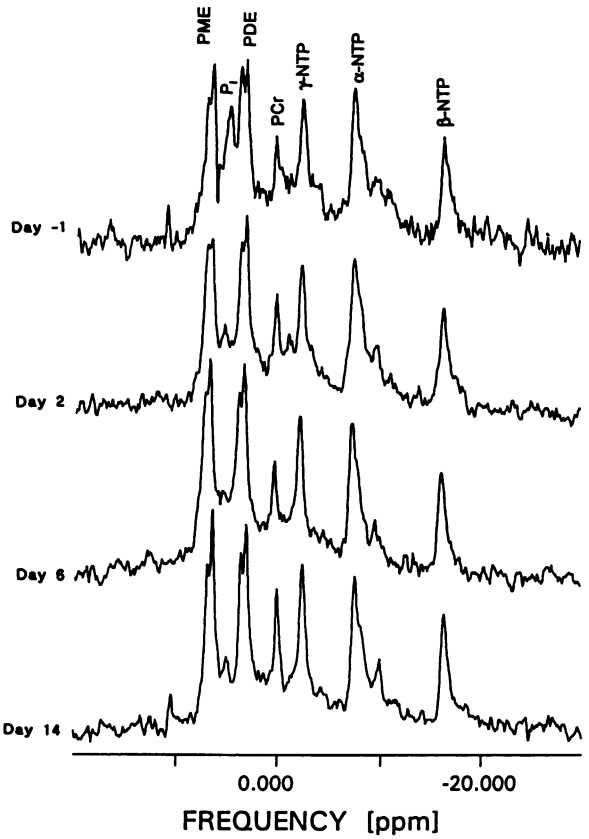

Fig. 5. ^{31}P MRS of a representative ZR75-1 tumor on days −1, 2, 6, and 14 after estrogen withdrawal.

Table 3 *Mean concentration of PCr and ATP in tumor tissue after 14 days of growth with or without 17β-estradiol*

		PCr (*n*), μmol/g	ATP (*n*), μmol/g	PCr:ATP
MDA-MB-231	$+E_2$	0.100 (3)	0.927 (4)	0.054
	$-E_2$	0.210 (4)	1.397 (5)	0.120
ZR75/LCC-3	$+E_2$	0.607 (11)[a]	0.193 (11)[a]	1.429[a]
	$-E_2$	0.796 (11)	2.240 (11)	0.363
ZR75-1	$+E_2$	0.489 (4)[a]	2.480 (4)	0.239[a]
	$-E_2$	1.179 (3)	1.626 (3)	0.687
MCF-7	$+E_2$	0.688 (4)[a]	2.246 (4)[a]	0.304
	$-E_2$	1.761 (4)	3.724 (4)	0.473

[a] $P < 0.05$.

the two estrogen-independent tumors) was significant ($P < 0.05$) when a *t* test was used, Fig. 7 shows considerable overlap between the SDs of PME:P_i, and it seems likely that the high predictive value of PME:P_i is mainly caused by the low PME:P_i ratio of the MDA-MB-231 tumors.

DISCUSSION

The present study is the first ^{31}P MRS report on the energy metabolic effect of estrogen withdrawal in human breast cancer xenografts on nude mice. The observed increase in the NTP:P_i ratio after estrogen withdrawal was closely related to estrogen dependence, since the lack of NTP:P_i increase was not only found in the *de novo* estrogen receptor-negative and estrogen-independent wild-type MDA-MB-231, but also in ZR75/LCC-3, selected from ZR75-1 for estrogen independence. The lack of NTP:P_i increase after estrogen withdrawal from ZR75/LCC-3 further corroborates that this phenomenon is in fact related to estrogen dependence. The underlying mechanisms are still unclear, but spectrophotometric analyses of tumor ATP and PCr content indicate that the observed changes in NTP:P_i are not caused by an increase in ATP concentration, more likely to a decrease in P_i concentration or decreased NMR visibility of the P_i molecules. Furthermore, we find the spectral appearance of the ^{31}P NMR spectrum, and particularly PME:P_i, to be a potential predictor of breast cancer estrogen dependence. Clinical studies are warranted to further elucidate the role of NMR spectroscopy in response prediction.

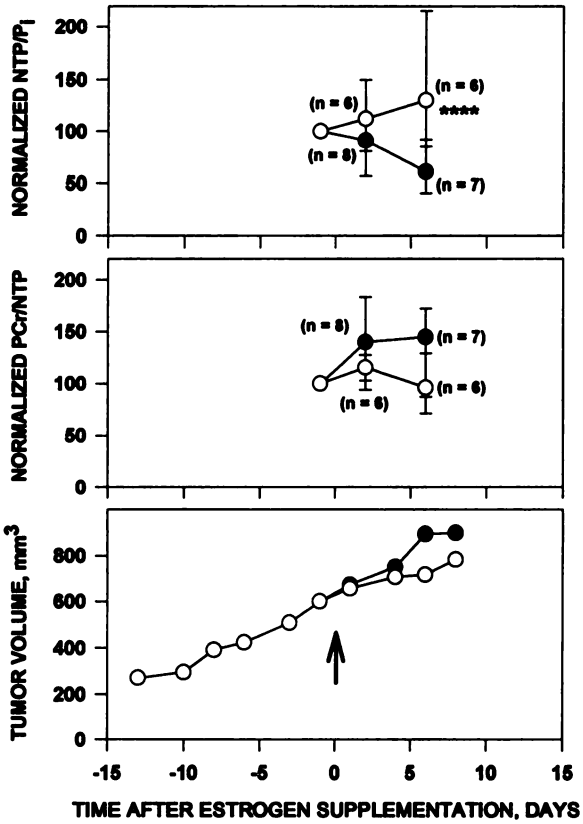

Fig. 6. Change in NTP:P_i (*top*), PCr:NTP (*middle*), and corresponding growth curves (*bottom*) of ZR75/LCC-3 tumors without 17β-estradiol stimulation (○) and after 17β-estradiol supplementation (●). *Error bars*, interquartile range. *Arrow*, day of estrogen supplementation. ***, $P < 0.1$.

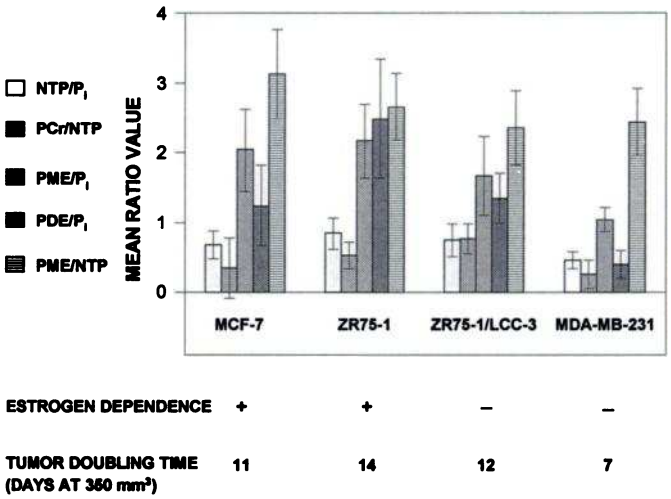

Fig. 7. Mean pretherapeutic ratios for each of the four examined tumor lines. *Error bars*, ±SD.

The effect of ovariectomy on energy metabolism detected by ^{31}P MRS in induced mammary tumors in rats has been studied by Rodrigues *et al.* (10), who found a significant increase in the PCr:NTP ratio in estrogen-sensitive tumors already 2 days after ovariectomy, whereas no change of this ratio was seen in response to ovariectomy in estrogen-insensitive tumors. As demonstrated in Figs. 1–6, we found a close correlation between estrogen dependence and energy metabolic (NTP:P_i) response to estrogen withdrawal. These findings are in concordance with those recently reported by Furman *et al.* (3, 4) in tamoxifen-treated MCF-7 tumors; a significant increase in the NTP:P_i ratio in response to the initiation of tamoxifen therapy was detected already after 4–7 days. In these studies performed in nude mice with intact ovaries, however, the estrogen pellet was removed when tamoxifen therapy was initiated. Consequently the observed increase in the NTP:P_i ratio may reflect estrogen deprivation as seen in the present study rather than initiation of tamoxifen therapy.

Whether the demonstrated changes in energy metabolic ratios after antihormonal therapy demonstrated by us and others (3, 4, 10) is caused by intracellular changes in metabolic rates or increased nutrient supply following stromal alterations has not been fully elucidated. Although a markedly decreased glycolytic rate following tamoxifen treatment has been demonstrated by ^{13}C MRS of the estrogen-dependent cell lines MCF-7 (3) and T47D (11) *in vitro*, central vascular collapse, as seen on magnetic resonance images after 24 h, was proposed as the origin of the abrupt spectral *in vivo* changes after estrogen withdrawal and initiation of tamoxifen therapy (4). The reported central necrosis and subsequent fibrosis in MCF-7 tumors is contrasting the data of Stubbs *et al.* (12), who found no histologically detectable changes in the tissue structure of induced mammary tumors after 2 days of estrogen deprivation. Furthermore, previous studies have indicated that tumor cell death in response to endocrine ablation cannot be attributed to vascular deficiency (13), and it has been demonstrated that an increased number of apoptotic cells are present in MCF-7 cells already 1 day after estrogen withdrawal (14). A difference in size between estrogen-stimulated and estrogen-depleted tumors would not explain the NTP:P_i increase, since in our study this observation was present already 2 days after estrogen withdrawal. Also, the acute NTP:P_i increase occurred in the growth-inhibited tumors, indicating that changes in tumor volume or localization was not the reason for the observed difference between growth-inhibited and control tumors.

We found no difference in the spectrophotometrically determined ATP concentration between estrogen-depleted and estrogen-supplemented ZR-75-1 tumors (Table 3). Consequently, a decrease in the P_i concentration was probably the explanation of the observed increase in the NTP:P_i ratio after estrogen withdrawal. This decrease in P_i could be caused by either increased washout due to improved tumor blood flow in the estrogen-depleted tumors or by a so-called compartmentation phenomenon: the intramitochondrial P_i pool is probably invisible by MRS. An increased mitochondrial uptake of P_i would decrease the cytoplasmatic (*i.e.*, visible) P_i concentration, and would consequently have increased the NTP:P_i ratio. This phenomenon has also been demonstrated in liver tissue, where a switch from a mainly glycolytic to a mainly gluconeogenetic state was followed by a decrease in NMR-detectable P_i and a corresponding increase in intramitochondrial P_i concentration (15). A similar compartmentation is not affecting the intracellular ATP visibility, which is relatively high (90%) and unaffected by the metabolic state of perfused liver tissue (16).

Increased ischemia in the growth-stimulated tumors may account for the difference in PCr content of the two groups of ZR-75-1 tumors (Table 3), as also reflected in the MRS data (Fig. 2). The PCr:NTP ratio is significantly decreased in the estrogen-stimulated compared to the estrogen-depleted tumors only on day 14 (*i.e.*, when the difference in size beween estrogen-stimulated and estrogen-depleted tumors is obvious). However, the fact that also the estrogen-independent ZR75/LCC-3 subline demonstrated a tendency toward decreased PCr concentration (Table 3) during estrogen stimulation, in spite of similar tumor sizes with and without estrogen stimulation, indicates a direct estrogen-mediated effect on the turnover of high-energy phosphates, possibly by regulation of creatine kinase activity.

Surprisingly, the ATP concentration of estrogen-depleted ZR75/LCC-3 tumors was 10-fold higher than in the continuously estrogen-stimulated tumors on day 14 after estrogen withdrawal. This finding may reflect a defect in the regulatory mechanisms of phosphate transfer between P_i, ATP, and PCr in estrogen-independent tumor cells. Still, no difference in ATP concentration was found between estrogen-supplemented and estrogen-depleted MDA-MB-231 tumors (Table 3). Although it may be that estrogen inhibits creatine kinase activity in estrogen-dependent tumors, it should be kept in mind that a down-regulation of enzyme activity does not change the steady-state concentration of either the substrate or the product, but only the conversion rate, provided that the system is in equilibrium. Recent studies have demonstrated a marked growth inhibitory effect on rat mammary tumors of dietary creatine and cyclocreatine, and PCr has been shown to inhibit several glycolytic enzymes (17), indicating a crucial role of creatine kinase and high-energy phosphates in the regulation of tumor growth.

PME:P_i turned out to be the pretherapeutic parameter most closely related to estrogen dependence (Table 2), and from the ^{31}P MRS appearance it has been possible with great certainty to discriminate between estrogen dependence/independence and to identify the individual tumors. PME are precursors in the biosynthesis of phospholipids (18). Other authors have proposed PME-related ratios as indicators of cancer and sensitivity to antiestrogens (19, 20) or chemotherapy (21) due to the presumed association of PME levels to increased synthesis of membrane phospholipids and cell turnover rate (22). A receptor-mediated regulatory effect of estrogen on the phospholipid metabolism might explain the observed differences in this study (Fig. 7). Our data also indicate that it is possible to reach an even higher predictability regarding estrogen dependency by including PCR:NTP, PDE:P_i, and PME:NTP (Table 2) in the analysis. The NTP:P_i ratio was correlated to PME:P_i and also to the tumor growth rate. Slow-growing tumors expressed a high NTP:P_i ratio and *vice versa* (Fig. 7). There was a general tendency in all tumors toward decreased NTP:P_i and PCr:NTP during tumor growth (Figs. 1–6). This relationship between energy metabolism and tumor growth is consistent with other observations of a decrease in NTP:P_i with increasing tumor size (2).

ACKNOWLEDGMENTS

We thank Ib Terkildsen and Ib J. Christensen for excellent assistance with the MRS recordings and statistical analyses, respectively.

REFERENCES

1. Griffiths, J. R., Bhujwalla, Z., Coombes, R. C., Maxwell, R. J., Midwood, C. J., Morgan, R. J., Nias, A. H. W., Perry, P., Prior, M., Prysor-Jones, R. A., Rodriguez, L. M., Stubbs, M., and Tozer, G. M. Monitoring cancer therapy by NMR spectroscopy. Ann. N. Y. Acad. Sci., *508:* 183–199, 1987.
2. de Certaines, J. D., Larsen, V. A., Podo, F., Carpinelli, G., Briot, O., and Henriksen, O. *In vivo* 31P MRS of experimental tumours. NMR Biomed., *6:* 345–365, 1993.
3. Furman, E., Rushkin, E., Margalit, R., Bendel, P., and Degani, H. Tamoxifen induced changes in MCF-7 human breast cancer: *in vitro* and *in vivo* studies using nuclear magnetic resonance spectroscopy and imaging. J. Steroid Biochem. Mol. Biol., *43:* 189–195, 1992.
4. Furman, E., Margalit, R., Bendel, P., Horowitz, A., and Degani, H. *In vivo* studies by magnetic resonance imaging and spectroscopy of the response to tamoxifen of MCF-7 human breast cancer implanted in nude mice. Cancer Commun., *3:* 287–297, 1991.
5. Clarke, R., Brünner, N., Thompson, E. W., Glanz, P., Katz, D., Dickson, R. B., and Lippman, M. E. The inter-relationships between ovarian-independent growth, tumor-

igenicity, invasiveness and antioestrogen resistance in the malignant progression of human breast cancer. J. Endocrinol., *122:* 331–340, 1989.

6. Kristjansen, P. E. G., Pedersen, E. J., Quistorff, B., Elling, F., and Spang-Thomsen, M. Early effects of radiotherapy in small cell lung cancer xenografts monitored by ^{31}P magnetic resonance spectroscopy and biochemical analysis. Cancer Res., *50:* 4880–4884, 1990.
7. Quistorff, B., and Chance, B. Simple techniques for freeze-clamping and for cutting and milling of frozen tissue at low temperature for the purpose of two or three dimensional metabolic studies *in vivo*. Anal. Biochem., *108:* 237–248, 1980.
8. Lowry, O. H., and Passonneau, J. V. A flexible system for enzymatic analysis. New York: Academic Press, 1982.
9. Spang-Thomsen, M., Clerici, M., Engelholm, S. A., and Vindelev, L. L. Growth kinetics and in vivo radiosensitivity in nude mice of two subpopulations derived from a single human small cell carcinoma of the lung. Eur. J. Cancer Clin. Oncol., *22:* 549–556, 1986.
10. Rodrigues, L. M., Midwood, C. J., Coombes, R. C., Stevens, A. N., Stubbs, M., and Griffiths, J. R. ^{31}P-nuclear magnetic resonance spectroscopy studies of the response of rat mammary tumors to endocrine therapy. Cancer Res., *48:* 89–93, 1988.
11. Neeman, M., and Degani, H. Metabolic studies of estrogen- and tamoxifen-treated human breast cancer cells by nuclear magnetic resonance spectroscopy. Cancer Res., *49:* 589–594, 1989.
12. Stubbs, M., Coombes, R. C., Griffiths, J. R., Maxwell, R. J., Rodrigues, L. M., and Gusterson, B. A. ^{31}P-NMR spectroscopy and histological studies of the response of rat mammary tumours to endocrine therapy. Br. J. Cancer, *61:* 258–262, 1990.
13. Gullino, P. M., Grantham, F. H., Losonczy, I., and Berghoffer, B. Mammary tumor regression. I. Physiopathologic characteristics of hormone-dependent tissue. J. Natl. Cancer Inst., *49:* 1333–1348, 1972.
14. Kyprianou, N., English, H. F., Davidson, N. E., and Isaacs, J. T. Programmed cell death during regression of the MCF-7 human breast cancer following estrogen ablation. Cancer Res., *51:* 162–166, 1991.
15. Eriksson, O., Pollesello, P., and Saris, N-E. The large intramitochondrial pool of inorganic phosphate of perfused rat liver is invisible by ^{31}P-NMR. 2nd IUBMB conference on biochemistry of cell membranes (Abstract). N. Perspect. Mitochon. Res., *2:* 61, 1993.
16. Masson, S., and Quistorff, B. The ^{31}P NMR visibility of ATP in perfused rat liver remains about 90%, unaffected by changes of metabolic state. Biochemistry, *31:* 7488–7493, 1992.
17. Miller, E. E., Evans, A. E., and Cohn, M. Inhibition of rate of tumor growth by creatine and cyclocreatine. Proc. Natl. Acad. Sci. USA, *90:* 3304–3308, 1993.
18. Ruiz-Cabello, J., and Cohen, J. S. Phospholipid metabolites as indicators of cancer cell function. NMR Biomed., *5:* 226–233, 1992.
19. Smith, T. A. D., Eccles, S., Ormerod, M. G., Tombs, A. J., Titley, J. C., and Leach, M. O. The phosphocholine and glycerophosphocholine content of an oestrogen-sensitive rat mammary tumour correlates strongly with growth rate. Br. J. Cancer, *64:* 821–826, 1991.
20. Twelves, C. J., Porter, D. A., Lowry, M., Dobbs, N. A., Graves, P. E., Smith, M. A., Rubens, R. D., and Richards, M. A. Phosphorus-31 metabolism of post-menopausal breast cancer studied *in vivo* by magnetic resonance spectroscopy. Br. J. Cancer, *69:* 1151–1156, 1994.
21. Dixon, R. M., Angus, P. W., Rajagopalan, B., and Radda, G. K. Abnormal phosphomonoester signals in ^{31}P MR spectra from patients with hepatic lymphoma. A possible marker of liver infiltration and response to chemotherapy. Br. J. Cancer, *63:* 953–958, 1991.
22. Daly, P. F., Lyon, R. C., Faustino, P. J., and Cohen, J. S. Phospholipid metabolism in cancer cells monitored by ^{31}P NMR spectroscopy. J. Biol. Chem., *262:* 14875–14878, 1987.